8.2 INVESTIGATIONS OF FLUX-PROFILE RELATIONSHIPS IN THE MARINE ATMOSPHERIC BOUNDARY LAYER DURING CBLAST

James Edson* and Robert Crofoot
Woods Hole Oceanographic Institution, Woods Hole, Massachusetts

Wade McGillis and Christopher Zappa
Lamont Doherty Earth Observatory, Palisades, New York

1. INTRODUCTION

Marine meteorologists and oceanographers have long relied on flux-profile relationships that relate the turbulence fluxes of momentum, heat and moisture (or mass) to their respective profiles of velocity, temperature, and water vapor (or other gases). The flux-profile or gradient-flux relationships are used extensively in numerical models to provide lower boundary conditions and to close the model by approximating higher order terms from low order variables.

The most commonly used flux-profile relationships are based on Monin-Obukhov (MO) similarity theory. MO similarity theory predicts that the non-dimensional gradient of velocity, temperature and humidity are universal functions of atmospheric stability

$$\phi_x(z/L) = \frac{\kappa z}{x_*}\frac{\partial X}{\partial z}$$

where $\partial X / \partial z$ and x_* are the gradient and scaling parameter for velocity, temperature, or humidity; z is the height above the surface, $\kappa = 0.4$ is von Karman's constant; and L is the MO length. These flux-profile relationships have been investigated during overland experiments since the mid-sixties. These experiments have generated a number of similar semi-empirical functions, with the most commonly used forms known as the Businger-Dyer formulae (Businger, 1988).

MO similarity is expected to hold and the derived parameterizations are expected to be universal as long as the assumptions that govern the MO similarity laws are valid: (1) a combination of mechanical and thermal forcing drive the turbulent exchange such that the relative strength of these two forces determines the characteristics of the near surface turbulence, (2) the scaling variables are independent of height in the surface layer, and (3) the turbulence statistics are stationary and horizontally homogeneous. The constant flux layer constraint is generally assumed to be valid in the lowest 10% of the unstable atmospheric boundary layer.

Near the ocean surface, however, wave induced forcing is expected to influenced the characteristics of the near surface flow. For example, recent investigations of the dimensionless shear over the ocean by Miller et al. (1997), Vickers and Mahrt (1999), and Smedman et al. (1999) report wave-induced effects that can cause substantial departure from MO similarity predictions. Therefore, the universality of these relationships to all surface layers is a current topic of intense debate. This paper provides results from our preliminary investigations of turbulent fluxes and their relationship with their associated mean profiles. This includes an investigation of wave related processes and their impact on the air-sea exchange and the vertical structure of the near surface flow over the ocean.

2. CBLAST

The objective of the Coupled Boundary Layers and Air-Sea Transfer Low Wind (CBLAST-LOW) experiment is to understand air-sea interaction and coupled atmospheric and oceanic boundary layer dynamics at low wind speeds where the dynamic processes are driven and/or strongly modulated by thermal forcing. The low wind regime will extends from the extreme situation where wind stress is negligible and thermal forcing dominates up to wind speeds where wave breaking and Langmuir circulations are also expected to play a role in the exchange processes.

Our goal is to make observations over a wide range of environmental conditions with the intent of improving our understanding of upper ocean and lower atmosphere dynamics and of the physical processes that determine both the vertical and horizontal structure of the marine boundary layers. The specific objectives of our research is to directly measure the vertical fluxes of momentum, heat and mass across the coupled boundary

* *Corresponding author address*: WHOI, J. Edson, MS #12, 98 Water Street, Woods Hole, MA, 02543; email: jedson@whoi.edu

layers (CBLs); to identify the processes that drive the flux and the CBL structure; to develop and evaluate parameterizations of the flux-producing processes; and to test the mean and variance budgets for momentum, heat, mass, and kinetic energy.

To achieve these objective, we deployed a fixed and profiler array of sensors on the Air-Sea Interaction Tower (ASIT). The ASIT is located 3.2 km south of Martha's Vineyard in the Atlantic and is directly cabled to shore via the Martha's Vineyard Coastal Observatory (MVCO). The ASIT was specifically designed to provide a low profile, fixed structure to minimize the adverse effects of flow distortion and remove the need for motion correction.

The air-side components deployed during the 2003 CBLAST IOP are shown in Fig. 1 and include sensor to measure wind velocity, air temperature, water vapor, precipitation, solar and infrared radiation, pressure, sea surface temperature, and wave height. A wide range of oceanographic sensors was deployed beneath the surface on the ASIT as well as on the ocean bottom. These sensors measured ocean currents, waves, penetrating solar radiation, salinity, and temperature.

Turbulence sensors were deployed at 6 levels to directly measure the fluxes of momentum, kinetic energy, temperature variance and sensible heat. The lowest 4 levels included sensors to measure the moisture variance and latent heat flux, while 2 levels were instrumented to measure the static pressure flux. A separate mast was deployed to support a moving package that measured the mean profiles of velocity, temperature and humidity.

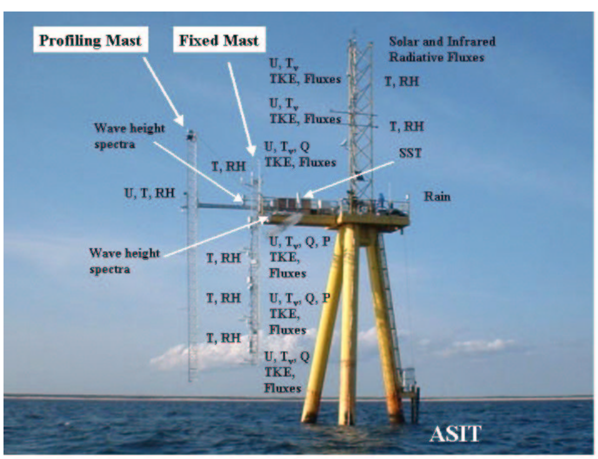

Figure 1. Experiment setup for the ASIT during CBLAST. The photo indicates where variables where measured on the met tower, fixed array, and profiling mast. The solar and infrared radiometers where measured 22-m above mean sea level.

3. ANALYSIS

The ASIT data is being used to investigate the relationship between the momentum, sensible heat, and latent heat fluxes and their associated mean profiles of velocity, potential temperature, and moisture, respectively. These investigations examine the validity of MO similarity theory as well as the departure from MOS due to the influence of the underlying wave field and other surface layer phenomena such as fog.

The TKE and scalar budget equations are used to investigate the physical processes that cause departure from classical law-of-the-wall behavior due to, e.g., stratification and energy flux to the wave field. The investigation hopes to provide improved parameterization of these processes for inclusion in numerical models of the marine atmospheric boundary layer.

3.1 *Bulk Aerodynamic Fluxes*

The bulk aerodynamic formula parameterize the sensible heat, latent heat, and momentum fluxes in terms of the more easily measured mean or bulk quantities and are expressed:

$$Q_h = \rho_a c_{pa} C_H S \left(T_s - \theta \right)$$
$$Q_e = \rho_a L_e C_E S \left(q_s - q \right)$$
$$\tau_i = \rho_a C_D S \left(u_{si} - u_i \right)$$

where θ, q, u_i and S are the average potential temperature, specific humidity, horizontal wind velocity in the ith direction, and instantaneous wind speed, respectively, at some height z; s denotes their surface values and $C_H, C_E,$ and C_D are the transfer coefficients for sensible heat (i.e. the Stanton number), latent heat (i.e. the Dalton number), and momentum (i.e. the drag coefficient) respectively.

The uncertainty in the determination of the momentum and scalar fluxes remains one of the main obstacles to accurate numerical forecasts in low to moderate wind conditions. For example, latent heat fluxes computed from data using direct covariance and bulk aerodynamic methods show that there is good agreement in unstable conditions when the latent heat flux values are generally positive. However, the agreement is relatively poor in stable conditions, particularly when the moisture flux is directed downward. If the direct covariance measurements are indeed accurate, then they clearly indicate that the bulk aerodynamic formula overestimate the downward moisture flux in stable conditions as shown in Fig. 2. Similar results were reported by Edson et al. (2000). As a result, comparisons of the Dalton number for unstable and stable conditions indicate a marked difference in value between the two stability regimes.

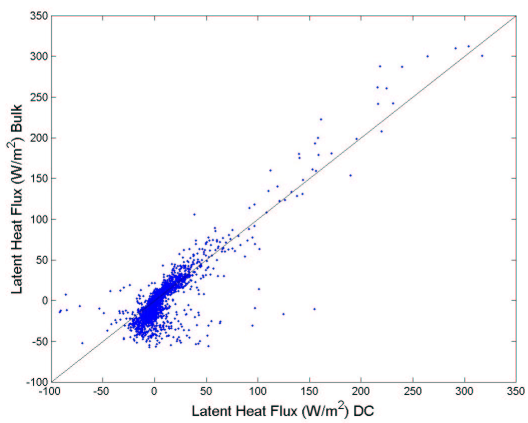

Figure 2. Comparison of direct covariance versus bulk aerodynamic fluxes measured from ASIT.

3.2 *The Dalton Number*

A case study of an eight-day period was recently completed by Lt. Crofoot to investigate the behavior of the transfer coefficients (Crofoot, 2004). During this eight-day period, the boundary layer was often characterized by light winds, a stably stratified surface layer and a swell dominated wave field. Additionally, the advection of warm moist air over cooler water resulted in fog formation and a downward flux of moisture on at least three occasions. The periods of downward moisture flux were associated with foggy conditions as shown in Fig. 3.

The primary objective of this investigation and that reported by Wang et al. (2004) is to investigate the cause of this shortcoming in the bulk formula under these conditions by examining the physical processes that are unique to these boundary layers. Particular attention is paid to the behavior of the Dalton number in a stable marine atmospheric boundary layer under foggy conditions. The Dalton numbers measured during the entire measurement campaign are shown in Fig. 4. The upper panel in this figure shows the Dalton numbers computed in stable, foggy conditions [using a criteria developed by Crofoot (2004)] are substantially lower than the TC3.0 algorithm (Fairall et al., 2003). As a result, the bin-averaged Dalton numbers computed under all stability conditions are biased low as shown in the lower panel. The stable data is still slightly lower than this parameterization and the modification reported by Edson (2002) even after removal of the foggy periods as shown in Fig. 5.

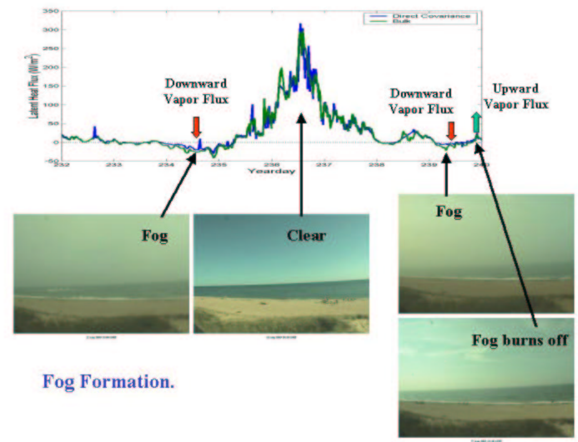

Figure 3. Time series of the latent heat fluxes and visual evidence for the presence of fog during periods of downward moisture flux.

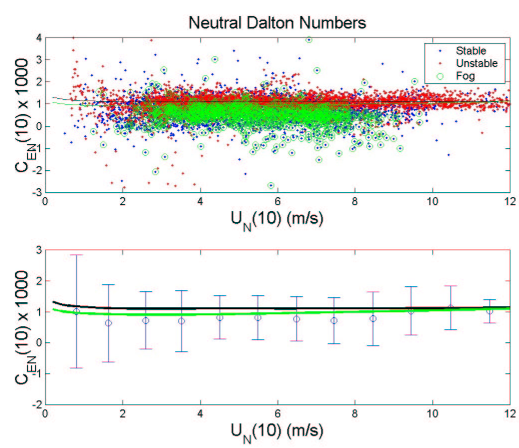

Figure 4. Measurements of the Dalton number plotted versus wind speed. Runs characterized by unstable, stable, and stable with fog are denoted by difference symbols. The black line is the TC3.0 parameterization while the green line is a modification reported by Edson (2002).

Our investigations are now focusing on the behavior of the flux-profile relations and their boundary conditions (i.e., the thermal "roughness" lengths) as measured from the ASIT during the fog-free periods. For example, the dimensionless moisture profiles computed during these periods are shown in Fig. 6. They show good agreement with the TC3.0 parameterization and the results given by Edson et al. (2004) for unstable conditions and slight differences from the stable situations. We will also continue our investigations of fog in collaboration with the COAMPS^{TM} modelers.

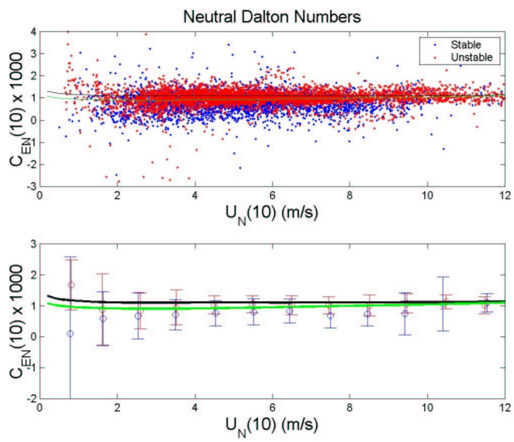

Figure 5. Dalton numbers calculated in the absence of fog. The unstable and stable cases have been bin-averaged separately.

3.3 *Stress-Swell interaction in Low Winds*

The drag coefficients computed from the CBLAST-Low data set show very good agreement with the TC 3.0 parameterization as shown in Fig. 7. While there is some disagreement between the data and the parameterization at the highest wind speed (likely due to coastal/shoaling wave effects), the most significant disagreement is found at the lowest wind speeds. At these lower wind speeds we expect naturally occurring variability and sampling problems to cause uncertainty in our direct covariance flux measurements. However, a number of recent studies by Sullivan et al. (2004) have indicated that some of this scatter may be driven by physical processes such as wind-stress-swell interaction.

Our preliminary investigations have focused on the eddy diffusivity for momentum

$$K_m(z) = -\overline{uw} / \frac{\partial U}{\partial z}$$

which is commonly parameterized using MO similarity theory as

$$K_m(z) = \frac{u_* \kappa z}{\phi_m(z/L)}$$

where ϕ_m is the dimensionless shear function. Direct measurements of the eddy diffusivity

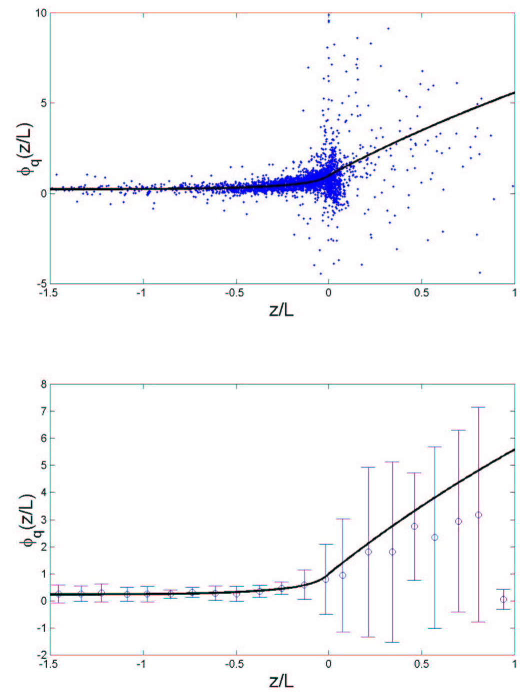

Figure 6. The dimensionless water vapor gradient plotted versus the stability parameter z/L.

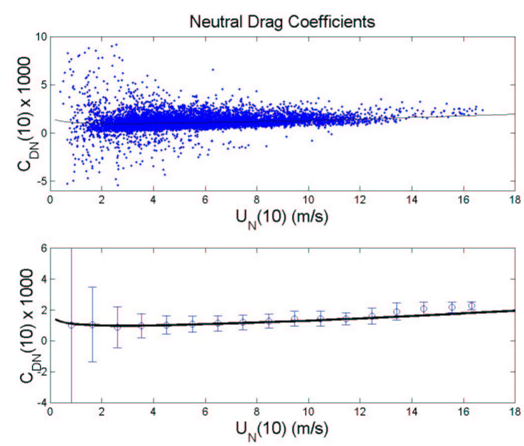

Figure 7. Drag coefficient estimates. The black line is the TC3.0 parameterization.

compared with this parameterization are shown in Fig. 8. The results in the lower panel have been bin-averaged in such a way that there are an equal number of points in each bin. This approach demonstrates that there is good agreement between the measurements and the parameterization for the vast majority of the data.

However, the plot also shows that the measured eddy diffusivities can be significantly larger than the parameterization under certain conditions; e.g., when the shear is smaller than expected given the magnitude of the stress.

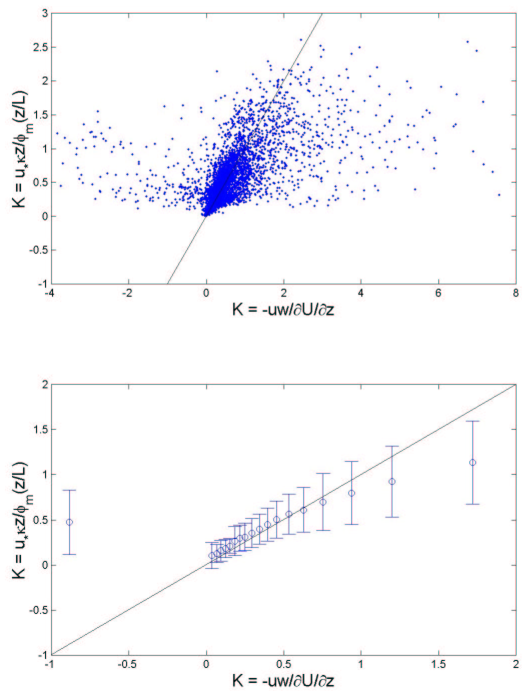

Figure 8. Direct estimates of the eddy diffusivity plotted versus a commonly used parameterization that relies on MO similarity functions.

The functional form of the dimension shear using in this parameterization is compared against measurements in Fig. 9. Although this function give good agreement in the mean with our data, closer examination of the measurements indicate that the anomalously large values of the eddy viscosity occur for the lowest values of ϕ_m as indicated by the red symbols in this figure. This is to be expected; however, it is somewhat surprising that many of these low values occur in near neutral conditions.

Our initial attempts to investigate the cause for these low values have been aided by the Large-Eddy Simulations of Sullivan et al (2004). The LES results clearly shown that fast moving swell in light winds can have a profound effect on the wind profile up to heights of O(10m). These conditions are know as old seas and are commonly found over the ocean whenever non-locally generated waves propagate into a low wind region or whenever local seas slowly decay as a storm moves out of the region. The former conditions were commonly observed during the CBLAST experiments.

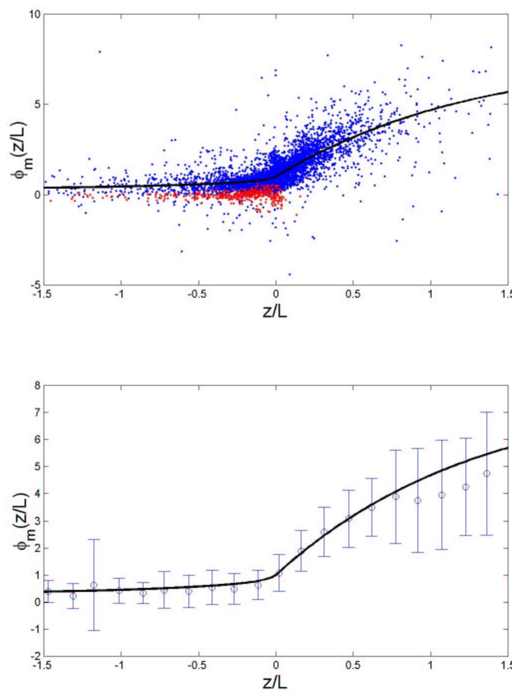

Figure 9. The dimensionless shear plotted versus the stability parameter z/L. The red points indicate measurements corresponding to eddy viscosities less than –0.2 or greater than 2.

To investigate the relationship of the velocity profiles to the state of the underlying sea, we limit our initial investigation to periods when the direction of the wind and dominant waves were within 25^o of each other. The velocity profiles during these periods have been normalized by their MO predictions

$$U_{MO}(z) = U(20) + \frac{u_*}{\kappa}[ln(z/20) - \psi_m(z/L) - \psi_m(20/L)]$$

where ψ_m is an integral form of ϕ_m. We then bin averaged by a wave age parameter c_p/U_{10}, where c_p is the phase speed of the dominant waves. Using this definition, previous studies have shown that fully developed (mature) seas have a wave age of approximately 1.2. Developing (young) seas have a smaller value, while decaying (old) seas have a larger value. As shown in Fig. 10, the bin-averaged profiles all depart from their MO similarity predictions as they approach the surface. The oldest wave show a velocity surplus while the youngest sea show a velocity deficit. However, this result is far from definitive as the results are very sensitive to, e.g., directional differences between the wind and waves. We are working to improve our directional wave estimates to improve our confidence in these results. Other effects that need to investigated further are related to fetch, flow distortion, sensor separation and flux divergence.

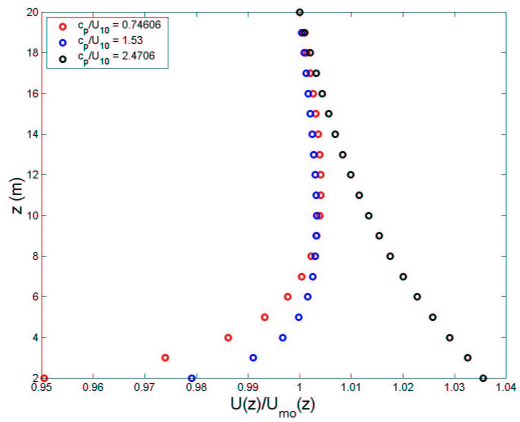

Figure 10. Velocity profiles normalized by their MOS predictions and bin-averaged into 3 wave age classes denoting young, mature, and old seas.

4. SUMMARY

An unprecedented data set was collected on both sides of the air-sea interface during CBLAST-LOW main experiment. These measurements are being used to investigate the processes that govern the exchange of momentum, heat, and mass across the CBLs. To date, we have focused our investigations on the traditional analysis of flux-profile relationship using MO similarity. However, these results have shown that there are significant differences between relationships developed over land versus those developed over the ocean. For example, we have already begun to shed light the physical processes governing, e.g., fog formation and stress swell interactions in low to moderate winds through a combination of process studies, numerical simulations, and mesoscale models. Our upcoming investigations will focus on the TKE and scalar variance budgets, and flux-profile relationships on both side of the air-sea interface. These studies will be conducted in collaboration with the oceanographers and numerical modelers. Continued investigations are expected to improve the predictive capabilities of a truly coupled COAMPS^{TM}.

Acknowledgements: This work was supported by the ONR under grants N00014-01-1-0029 and N00014-01-1-0081. Lt. Robert Crofoot's participation in CBLAST was supported by the U.S. Navy.

REFERENCES

Businger, J. A., 1988: A note on the Businger-Dyer profiles, *Bound.-Layer Meteorol.*, *42*, 145-151.

Crofoot, R. F., 2004: Investigations of scalar transfer coefficients in fog during the Coupled Boundary Layers and Air-Sea Transfer experiment: A case study, *M.S. Thesis*, WHOI/MIT Joint Program.

Edson, J., 2002: Air-sea fluxes in high winds, Ocean Sci. Mtg., Honolulu, HI, OS51C-01.

Edson, J. B., et al., 2000: Downward Flux of Moisture over the Ocean, *Proc. 14th Symp. on Boundary Layers and Turbulence*, Aspen, CO, Amer. Meteor. Soc., 511-513.

Edson, J. B., C. J. Zappa, J. A. Ware, W. R. McGillis, and J. E. Hare, 2004: Scalar flux profile relationships over the open ocean," *J. Geophys. Res.*, in press.

Fairall, C. W., E. F. Bradley, J. E. Hare, A. A. Grachev, J. B. Edson, 2003: Bulk parameterization of air–sea fluxes: Updates and verification for the COARE algorithm, *J. Climate*, *16*, 571–591.

Miller, S. D., et al., 1997: Wind and turbulence profiles in the surface layer over the ocean, Extended Abstracts, *Proc. 12th Symp. on Boundary Layers and Turbulence*, Vancouver, BC, Amer. Meteor. Soc., 308-309.

Smedman, A., U. Högström, H. Bergström, A. Rutgersson, K. K. Kahma, and H. Pettersson, 1999: A case study of air-sea interaction during swell conditions, *J. Geophys. Res.*, *104*, 25833-25851.

Sullivan, P. P., et al., 2004: Large-eddy simulations and observations of wave-driven boundary layers, *Proc. 16th Symp. on Boundary Layers and Turbulence*, Portland, ME, Amer. Meteor. Soc., This Volume.

Vickers, D. and L. Mahrt, 1999: Observations of non-dimensional wind shear in the coastal zone, *Quart. J. Roy. Met. Soc.*, *125*, 2685-2702.

Wang, S., et al., 2004: Evaluation of COAMPS^{TM} real time forecast for CBLAST-Low summer experiments 2002/2003, *Proc. 16th Symp. on Boundary Layers and Turbulence*, Portland, ME, Amer. Meteor. Soc., This Volume.